



Modelling rotavirus concentrations in rivers: Assessing Uganda's present and future microbial water quality

Daniel A. Okaali^{a,*}, Carolien Kroeze^a, Gertjan Medema^b, Peter Burek^c, Heather Murphy^d, Innocent K. Tumwebaze^e, Joan B. Rose^f, Matthew E. Verbyla^g, Sowed Sewagudde^h, Nynke Hofstra^a

^a Water Systems and Global Change Group, Wageningen University & Research, Wageningen, The Netherlands

^b KWR Watercycle Research Institute, Nieuwegein, The Netherlands

^c International Institute for Applied Systems Analysis, Laxenburg, Austria

^d Department of Pathobiology, Ontario Veterinary College, University of Guelph, Guelph, ON, Canada

^e School of Architecture, Building & Civil Engineering, Loughborough University, Loughborough, United Kingdom

^f Department of Fisheries and Wildlife, Michigan State University, East Lansing, MI, USA

^g Department of Civil, Construction and Environmental Engineering, San Diego State University, San Diego, CA, USA

^h Directorate of Water Resources Management, Ministry of Water and Environment, Kampala, Uganda

ARTICLE INFO

Keywords:

Sanitation
Surface water
Waterborne pathogens
Scenarios
Climate change

ABSTRACT

Faecal pathogens can be introduced into surface water through open defecation, illegal disposal and inadequate treatment of faecal sludge and wastewater. Despite sanitation improvements, poor countries are progressing slowly towards the United Nation's Sustainable Development Goal 6 by 2030. Sanitation-associated pathogenic contamination of surface waters impacted by future population growth, urbanization and climate change receive limited attention. Therefore, a model simulating human rotavirus river inputs and concentrations was developed combining population density, sanitation coverage, rotavirus incidence, wastewater treatment and environmental survival data, and applied to Uganda. Complementary surface runoff and river discharge data were used to produce spatially explicit rotavirus outputs for the year 2015 and for two scenarios in 2050. Urban open defecation contributed 87%, sewers 9% and illegal faecal sludge disposal 3% to the annual 15.6 log₁₀ rotavirus river inputs in 2015. Monthly concentrations fell between -3.7 (Q5) and 2.6 (Q95) log₁₀ particles per litre, with 1.0 and 2.0 median and mean log₁₀ particles per litre, respectively. Spatially explicit outputs on 0.0833 × 0.0833° grids revealed hotspots as densely populated urban areas. Future population growth, urbanization and poor sanitation were stronger drivers of rotavirus concentrations in rivers than climate change. The model and scenario analysis can be applied to other locations.

1. Introduction

Rotavirus (Group A) predominantly causes acute gastroenteritis in children below 5-years worldwide (Tate et al., 2016). An infected person excretes between 10¹⁰ to 10¹² particles per gram of faeces (Bishop, 1996). Individuals get infected through the ingestion of contaminated water, food or person-to-person contact (Rodrigues et al., 2002; Tate et al., 2009). Open defecation, indiscriminate disposal and the inadequate treatment of wastewater and faecal sludge can introduce such pathogens to surface water (Caceres et al., 1998; Williams and Overbo, 2015). These faecal contamination pathways are common in densely

populated urban slums (Katukiza et al., 2012; Kayima et al., 2010).

Progress monitoring of the 2030 Sustainable Development Goals (SDGs) indicated 9 out of 10 countries with <5% basic sanitation coverage in 2015. A majority of the 2.3 billion people without basic sanitation use unimproved technologies like unlined pit latrines, hanging or bucket toilets, or practice open defecation (WHO and UNICEF, 2017). In Uganda, our case study, 75% of the population mostly uses unsafely managed onsite sanitation (pit latrines and septic tanks) while the rest practices open defecation. The coverage of sewerage systems is lower than 1% and is limited to larger cities (Okaali and Hofstra, 2018). During heavy rainfall, unlined pit latrines and

* Corresponding author.

E-mail addresses: daniel.okaali@wur.nl, cdnadan@gmail.com (D.A. Okaali).

<https://doi.org/10.1016/j.watres.2021.117615>

Received 21 April 2021; Received in revised form 2 August 2021; Accepted 24 August 2021

Available online 28 August 2021

0043-1354/© 2021 The Authors.

Published by Elsevier Ltd.

This is an open access article under the CC BY-NC-ND license

(<http://creativecommons.org/licenses/by-nc-nd/4.0/>).

stormwater drains can overflow and their contents wash out, introducing high concentrations of pathogens into the environment (Berendes et al., 2018; Peal et al., 2020; Schoebitz et al., 2016).

Modelling microbial water quality can be a first step towards informing sanitation management decisions in data-poor areas (Hofstra et al., 2019; van Vliet et al., 2019). The models can study pollutant sources, identify hotspots and assess the impacts of environmental change. Our study used the process-based Global Water Pathogens (GloWPa) model which simulates global, regional and national scale outputs (Hofstra et al., 2013; Kiulia et al., 2015; Vermeulen et al., 2019). Generally, the model explores sanitation service chain pathways for pathogen sources and then conceptualizes operational sink-to-source processes. Point source emissions are estimated from sewerage systems and urban open defecation, while diffuse source emissions are from rural open defecation. Onsite sanitation technologies are treated as non-sources. However, not all faeces from onsite sanitation can be safely contained (Schoebitz et al., 2016; Williams and Overbo, 2015). Unsafely managed onsite technologies in unplanned densely populated settlements have also been linked to microbial surface and groundwater contamination (Berendes et al., 2018; Katukiza et al., 2013; Murungi and van Dijk, 2014).

Fate and transport studies highlight the role of hydrological flows in mobilising pathogens from land to water by correlating disease outbreaks to rainfall events (Ferguson et al., 2003; Mawdsley et al., 1995; Schäfer et al., 1998). In surface water, pathogens can die off from stressors like temperature, salinity, sunlight, presence of bacteria, organic matter and sedimentation (Pinon and Vialette, 2018). Therefore, integrating microbial loss-survival components can improve model reliability (Mawdsley et al., 1995). Moreover, surface runoff and discharge data can be used to quantify microbial streamflow concentrations. Consequently, microbial exposure risk can be predicted and the disease burden estimated when population exposure behaviours are understood.

Future climate change is predicted to increase diarrhoeal disease burden, particularly in low and middle-income countries, under socio-economic scenarios of continued fossil fuel use (IPCC, 2014; Levy et al., 2018). However, such studies mostly use historical diarrhoeal disease patterns. An integrated modelling approach combining socio-economic development and climate change impacts could provide new knowledge on future microbial water quality and the resulting diarrhoeal disease burden (Hofstra, 2011; Hofstra et al., 2019). Thus far, such studies are grossly limited.

Our study aimed to simulate spatially explicit rotavirus river concentrations, accounting for onsite sanitation technologies (pit latrines and septic tanks) in addition to sewerage systems (offsite) and open defecation; and to analyse the impacts of future sanitation management, population, urbanization and climate change on rotavirus concentrations. The GloWPa-Rota C2 model presented here simulates rotavirus concentrations in rivers, with rotavirus as an exemplar waterborne pathogen. The model and scenario analysis were applied to Uganda as a case study with prevalent sanitation challenges. Pathogen sources, hotspots, and future impacts of population growth, sanitation management, and climate change on rotavirus concentrations in Uganda's rivers were explored. The model can be applied to other countries and used for monitoring SDG6.3 progress.

2. Methods

We build on the GloWPa-Rota H1 (Kiulia et al., 2015; Okaali and Hofstra, 2018) and GloWPa-Crypto C1 (Vermeulen et al., 2019) models in this paper. Detailed model descriptions can be found in these sources. Here, we focused on modifications and input variable changes. Table S1 and Figure S1 in Supplementary materials (S) presents the models, variables and literature resources applied in this paper. Briefly, the GloWPa-Rota H1 model simulates global human rotavirus emissions reaching surface water while the GloWPa-Crypto C1 model simulates

global human and animal *Cryptosporidium* concentrations in rivers. Both models compute annual spatial outputs from human or animal populations, faecal pathogen shedding, sanitation coverage, storage survival and wastewater treatment removal represented on $0.5 \times 0.5^\circ$ grid resolution. Emissions are calculated from point (sewerage systems and urban open defecation), and diffuse (rural open defecation or animal) sources. For the current paper, onsite sanitation technologies were added to the existing GloWPa-Rota H1 model (Section 2.1) to produce human emissions for Uganda's 112 districts. Rotavirus transported by surface runoff, the environmental survival fraction, and river discharge data were used to build the GloWPa-Rota C2 model for simulating concentrations (Section 2.2). Surface runoff and discharge are outputs from the distributed Community Water model (CWatM) for water resources assessment cropped to within Uganda's geographical extent. Prior to our study, CWatM was used to assess how water demand and availability evolve in the extended Lake Victoria basin using socio-economic and climate change scenarios for the year 2050 (Burek et al., 2020).

2.1. The GloWPa-Rota H2 model: Onsite sanitation integration and simulating rotavirus river inputs

The GloWPa-Rota H1 model simulated annual human rotavirus emissions from sewerage systems and open defecation (Kiulia et al., 2015; Okaali and Hofstra, 2018), summing human emissions from urban and rural populations (Section S2). In the current study, onsite sanitation was added into the existing GloWPa-Rota H1 framework by interpreting faecal sludge management practices in Uganda. Unlike in Kiulia et al., where a constant fraction transported by surface runoff was used, we computed diffuse emissions by calculating grid-to-grid land retention fractions using grided surface runoff data. The sum of point and diffuse source emissions was thereafter referred to as 'river inputs.'

Although faecal sludge management data may be limited, excluding onsite sanitation technologies for areas with a large coverage is unrealistic. In an example of Kampala, Uganda, faecal sludge disposal events can variably include the appropriate emptying and transport to treatment, illegal dumping into water or land and the flushing into stormwater channels (Murungi and van Dijk, 2014; Schoebitz et al., 2016; Tsinda et al., 2015). Therefore, differentiated onsite sanitation management events and pathways in Figure 1 were integrated into the new GloWPa-Rota H2 model as:

$$OS_{u,r} = P_{u,r} \times f_{u,r,age} \times f_{u,r,em} \times V_p \times f_{\bar{x}} \times (f_{dl} + f_{dw} + f_{fw} + f_{et} \times (1 - f_{rem}))_{u,r} \quad (1)$$

Where $OS_{u,r}$ is the urban or rural rotavirus river inputs from onsite sanitation, $P_{u,r}$ is the urban or rural district population, $f_{u,r,age}$ is the fraction of the urban or rural age group (<5, >5 years), $f_{u,r,em}$ is the faecal sludge fraction emptied from pit latrines and septic tanks in urban or rural areas, V_p is the rotavirus shedding calculated by multiplying rotavirus excretion and incidence rates in the age group, and $f_{\bar{x}}$ is the average survival fraction during storage time. The illegal faecal sludge disposal proportions are: f_{dl} for the fraction emptied and disposed on land, f_{dw} into water, and f_{fw} is flushed into waterways. Appropriately disposed faecal sludge, f_{et} , is emptied and transported to wastewater treatment facilities, and f_{rem} is the fraction of rotavirus removed by the treatment type and stage (Section S2).

Occurrences for illegal faecal sludge disposal are unknown. A study in Kampala estimated 46% of faecal sludge as unsafely managed and 54% safely managed (Schoebitz et al., 2016). From Murungi and van Dijk (2014); Schoebitz et al. (2016) and Tsinda et al. (2015), the greatest proportion is flushed out such as during rainfall events. Therefore, we assumed the ratios $f_{dl} = 5\%$, $f_{dw} = 15\%$ and $f_{fw} = 80\%$ constitute the 46% unsafely managed waste. A fraction of faecal sludge was assumed as not emptied and was excluded as a non-source (Figure 1: Remaining contained). For all urban areas, unsafe faecal sludge management was

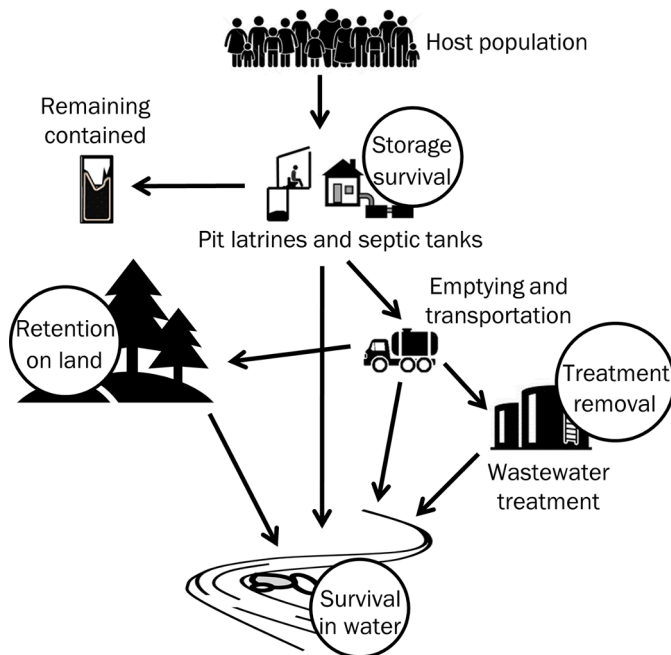


Fig. 1. Adding onsite sanitation to the GloWPa H2 model: modelled pathogen pathways (arrows) and die-off or retention processes (circles) during the collection, storage, conveyance, treatment and disposal of faecal sludge.

assumed to include illegal flushing and dumping into water or land while safe faecal sludge management included emptying followed by treatment. A common practice in rural areas due to the available space is digging a new pit elsewhere. Therefore, rural illegal disposal activities were excluded.

The GloWPa-Rota H2 model assigned both offsite and post-treatment onsite emissions to respective grid location of the 25 wastewater treatment plants, instead of gridded averages in the GloWPa-Rota H1 model. Each wastewater treatment plant was assigned an output fraction depending on its configuration (activated sludge or stabilization ponds) and capacity.

The average storage survival fraction of rotavirus was calculated from the rate order exponential decay basing on the *Cryptosporidium* animal manure storage survival estimation in Vermeulen et al. (2017). Rotavirus decay day^{-1} during storage time (K_{pit}) was obtained from a systematic literature review of pathogen survival in untreated excreta (Fleming, 2017).

In Vermeulen et al. (2019), surface runoff was used to calculate grid-based river inputs. Because runoff does not mobilise all pathogens, a significant fraction is retained in the soil and vegetation. Vermeulen et al. (2019) and our literature review (Section S3) found no standard for modelling microbial transport from land to rivers. Consequently, we calculated the retained fraction from diffuse sources using surface runoff data. Upper and lower retention values from literature were assigned naturalized global runoff ranges such that grids with high runoff received lower retention values and vice versa (Section S3, Table S2). Diffuse emissions were multiplied with the runoff fraction and added to point emissions to obtain grid-based annual rotavirus river inputs.

2.2. The GloWPa-Rota C2 model: Simulating rotavirus concentrations in rivers

Like Vermeulen et al. (2019), grid-to-grid pathogen survival in rivers for a particular month was estimated from literature and the total loss rate coefficient developed by summing rate order die-offs due to temperature and solar radiation, before the loads were routed downstream. Sedimentation in water was excluded as being implausible for rotavirus.

2.2.1. Temperature dependent decay of rotavirus in fresh surface water

Literature on infectivity inactivation of rotavirus in fresh surface waters was reviewed. Section S4 and Table S3 present the review approach and the few resources meeting our criteria. Recorded data ($K_{T,i}$ day^{-1}) was used to obtain the first-order decay rate in equation below.

$$K_{T,i} = \beta_0 + \beta_1 T_i, \quad (2)$$

with K_T being the gridded temperature-dependent decay rate at water temperature T ($^{\circ}\text{C}$) in month i ($\beta_0 = -0.0397$, $\beta_1 = 0.0089$, $n = 20$, $P < .001$). T was obtained from CWatM.

2.2.2. Sunlight dependent decay of rotavirus in fresh surface water

A few studies from literature reviewed on rotavirus solar inactivation in fresh surface waters or synthetic aqueous conditions are assembled in Table S4 (Section S5). Decay versus insolation values was estimated by fitting a line into the data for full spectrum irradiation in solutions containing sensitizers (Figure S4). Solar radiation dependent decay was then modelled using the Thomann & Mueller (1987) equation:

$$K_{R,i} = \frac{k_i I_{A,i}}{k_e Z_i} (1 - e^{-k_e Z_i}) \quad (3)$$

Where K_R is the depth-averaged solar radiation dependent decay (day^{-1}), k_i is the proportionality coefficient ($\text{m}^2 \text{KJ}^{-1}$), I_A is the average daily surface insolation ($\text{KJm}^{-2} \text{day}^{-1}$), k_e is the solar radiation attenuation or light extinction coefficient (m^{-1}), and Z is the average river depth (m) for month i . I_A and Z are obtained from CWatM.

Kirk (1981) and Lee et al. (2005) showed how k_e can be modelled using inherent optical properties of water like absorption, reflection and refraction. Consequently, the relation between downwelling scalar irradiance ($E_d(z_0)$) at water depth 0 and irradiance at a certain depth z ($E_d(z_1)$) for photosynthetically available radiation can be described as:

$$E_d(z_1) = E_d(z_0) e^{-k_e(z_1 - z_0)} \quad (4)$$

In general k_e increases with water depth z , and can be averaged over a mixed water column as shown in equation 5 (Lee et al., 2005). \bar{k}_e is the average attenuation coefficient (m^{-1}) between z_0 at the surface and at depth z_1 .

$$\bar{k}_e(z_0 \leftrightarrow z_1) = \frac{1}{z_1 - z_0} \ln \frac{E_d(z_0)}{E_d(z_1)} \quad (5)$$

The euphotic depth (z_{eu}) was used to represent z_1 . z_{eu} is the distance from the surface to the point where light penetration reaches just 1% of the insolated surface radiation (Kirk, 1994, 1981). At z_0 , this amount is 100% ($E_d(z_0)$). Solar radiation penetrating beyond this point may be inadequate for photosynthesis. We assumed the same for virus decay. Therefore, $z_1 = z_{eu}$, with $z_0 = 0$ at the surface, $E_d(z_0) = 100\%$ and $E_d(z_1) = 1\%$. Two studies support this approach, arguing that calculating depth-averaged light extinction is more useful than obtaining point values in the water column (Lee et al., 2005; McCormick and Højerslev, 1994). The new depth and radiation values were substituted into equation 5, making k_e dependent on z_{eu} ($\bar{k}_e = 4.6052/z_{eu}$). Typical z_{eu} ranges in Uganda's rivers were not found. However, 67 z_{eu} data points were obtained from two studies on Murchison Bay, Fielding Bay and Napoleon Gulf along the northern shores of Lake Victoria between 2001 and 2004, which predicted the mean monthly \bar{k}_e profile (Figure S5). Finally, we substituted for K_R , \bar{k}_e , z and I_A to obtain the coefficient k_i at any value of the former parameters ($k_i = 4.71 \times 10^{-5}$).

2.2.3. Routing of rotavirus concentrations in rivers

Prior to routing, the GloWPa-Rota C2 model used streamflow networks from CWatM's gridded flow direction and flow accumulation outputs. River depth (m), width (m) and flow velocity ($\text{m}^3 \text{s}^{-1}$) were calculated from the CWatM's naturalized discharge ($\text{m}^3 \text{s}^{-1}$), with water demand for domestic, agriculture, livestock and industry excluded,

enabling the estimation of water residence time. Residence time per grid cell is the river length (straight-line river stretch between adjacent grids) divided by flow velocity. During residence time, more water accumulated in a grid cell, depending on the number of surrounding to-draining cells. Routing of river inputs started from low accumulation cells, such that the next grid cell received additional loading from the previous cell. Total loading for the current grid cell was calculated and adjusted for environmental survival using the loss rate coefficient as:

$$L_{i,n} = (Diff_i + Pnt_i + L_{i,n-1}) * e^{-K_i t_i} \quad (6)$$

Where $L_{i,n}$ is the loading per month in month i , in a grid with flow accumulation number n from diffuse ($Diff_i$) and point (Pnt_i) sources, $L_{i,n-1}$ is the routed loading from the previous grid to the current grid, K_i is the total loss rate coefficient and t_i is the residence time in days. K_i depends on pathogen environmental survival presented earlier. Total monthly concentrations were then calculated from discharge (Q_i) as:

$$C_i = \frac{L_i}{Q_i} \quad (7)$$

2.3. Model sensitivity

Mathematical, nominal and exclusion tests were performed in the sensitivity analysis. In the mathematical approach, values were changed by increasing or decreasing variables with the same proportion. For nominal sensitivity, variables were given upper and lower values based on the indicated literature. The GloWPa-Rota C1 median and mean concentrations output changes were then investigated for sensitivity to changes in input variables (see details in Section S6).

2.4. Scenario analysis

2.4.1. Narratives and data sources

Baseline and scenario GloWPa-Rota C2 model input data were representative for approximately the years 2015 and 2050, respectively. These data included urban and rural populations, sanitation coverage, faecal sludge management, wastewater treatment proportions (Table S6) and climate change data (surface runoff, water temperature, solar radiation and river discharge) from CWatM. Scenario inputs were based on two Shared Socio-economic Pathways (SSPs) and three Representative Concentration Pathways (RCPs). SSPs are the five alternative narratives for future socio-economic development, assessing climate change impacts, vulnerabilities, adaptation and mitigation (Riahi et al., 2017). The RCPs are the four greenhouse gas concentration trajectories developed by the global climate modelling community with radiative forcings 2.6, 4.5, 6.0 and 8.6 Wm^{-2} , spanning up to the year 2100 (van Vuuren et al., 2011).

The CWatM outputs for SSP1 and SSP2 represented two plausible futures in 2050 for the extended Lake Victoria Basin (Tramberend et al., 2020). SSP1 is the 'sustainability' narrative, describing optimistic prospects on socio-economic development, population growth and urbanization. Inclusive development and environmental limit awareness lead towards achieving SSP1 climate targets. SSP2 is the 'middle-of-the-road' narrative with a near-customary pattern, dominated by unequal socio-economic growth. RCPs for the extended Lake Victoria basin are simulations from General Circulation Models (GCMs) (Tramberend et al., 2020). Four GCMs from the Coupled Model Intercomparison Project 5 (CMIP5) (Flato et al., 2013) are used in the Inter-Sectoral Impact Model Intercomparison Project (ISI-MIP) (Frieler et al., 2016). These GCMs were bias-corrected to represent the current climate, and out of the four, HadGEM2-ES and MIROC5 were selected as the most feasible GCMs for the East African region (Tramberend et al., 2020).

Gridded RCPs 2.6, 4.5 and 6.0 data for surface runoff, water temperature, solar radiation and river discharge were used as climate inputs into the GloWPa-Rota C2 model for 2050. Urban and rural populations

for Uganda were compiled from the SSPs public database (Riahi et al., 2017). We assumed urban and rural grids grow proportionally from the baseline such that no new densely populated grids are formed and the current urban or rural grids remain in 2050. Detailed data for population and sanitation coverage assumptions, and climate change analysis are provided in Section S7.

3. Results

3.1. Rotavirus sources and river inputs in Uganda's surface waters in 2015

The GloWPa-Rota H2 model simulated human rotavirus river inputs from sanitation systems for the baseline year 2015. Urban open defecation contributed a total of 15.5 (87%), sewerage 14.5 (9%), onsite 14.1 (3%) with almost all the share of 92% coming from illegal flushing, and rural open defecation 13.3 (1%) \log_{10} particles per year to surface water annually. Hotspots were identified as the various densely populated centres across the country, with outputs between 12.0 and 14.5 \log_{10} particles per year. Overall, population density and sanitation coverage accounted for the spatial distribution of river inputs (Figure 2 (a)). Districts with higher emissions also identified in Okaali & Hofstra (2018) included Kampala, Wakiso, Masaka and Iganga, had an average of 14 \log_{10} particles per year. However, point source emissions dominated diffuse source emissions by 99%.

3.2. Uganda river concentrations of rotavirus in 2015

Monthly rotavirus river concentrations from the GloWPa-Rota C2 model mostly fell between -5 and 5 \log_{10} particles per litre, with medians between -0.3 and 2 \log_{10} particles per litre of surface water. Figure 2(b) shows annual mean rotavirus concentrations in small and large rivers across the country at a spatial resolution of $0.0833 \times 0.0833^\circ$ grids. Most of the routed grid-to-grid concentrations were transported downstream, attributable to the simulated monthly K_T and K_R and the high survival fractions (Figure S7 and S8). Lake Victoria was excluded because the model was assumed less representative for large water bodies, arising from among others, uncertainties in estimating retention time, travel distance and the virus loss-survival fraction. Grids with discharge values below $1 \text{ m}^3\text{s}^{-1}$ were also excluded, because the model would predict unreasonably high concentrations. Monthly differences in concentrations were largely due to changes in river discharge, as seen in the examples of July (dry) and November (wet) in Figure 2(c) and 2(d) respectively. For these months, differences were observable in the south western parts of the country, likely resulting from the seasonal wet-to-dry shifts relative to other parts of the country.

3.3. Sensitivity analysis of the GloWPa-Rota C2 model

The GloWPa-Rota C2 median and mean concentrations outputs increased significantly by 2 and 10 orders of magnitude when rotavirus incidence and excretion rates were doubled or increased by 1 \log_{10} , respectively. While the influences of changes in temperature and solar dependent decays were limited, excluding K_{pit} alone contributed 2.76 (median) and 2.99 (mean) orders of magnitude to outputs, respectively. However, the model mostly accommodated other given variable fluctuations. For instance, median and mean results were largely unchanged whether faecal sludge is emptied yearly or every 10 years, registering limited to no interaction between K_{pit} and the faecal sludge emptying ranges. Varying log land retention, surface runoff and maximum and minimum monthly runs for river discharge, runoff, water temperature and solar radiation registered limited to no output changes. Detailed results are discussed in Section S6.

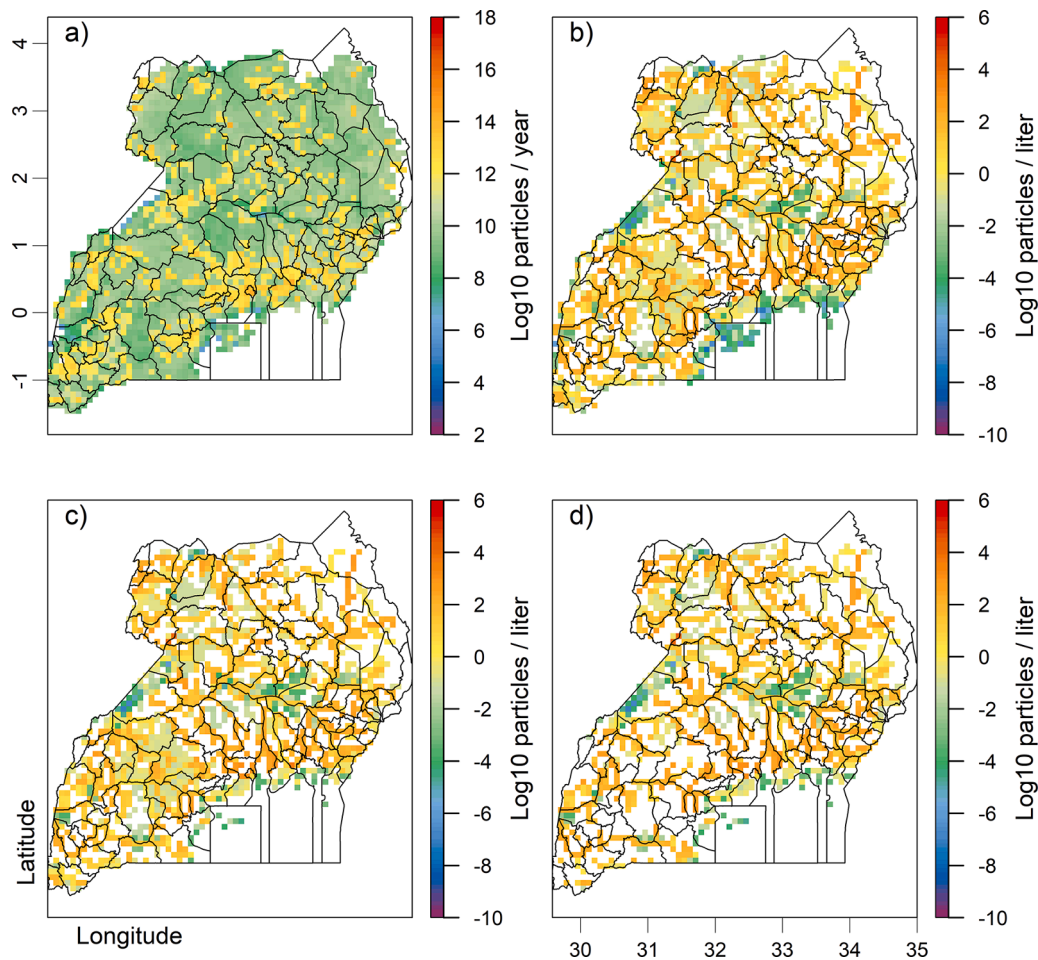


Fig. 2. Uganda’s spatially-explicit rotavirus loadings into surface water in 2015. Respectively, (a): river inputs,(b): mean annual river concentrations, (c): concentrations in November (wet), and (d): July (dry), simulated at a $0.0833 \times 0.0833^\circ$ grid resolution.

3.4. Rotavirus concentrations in Uganda’s rivers in 2050

Rotavirus river concentrations were lower in SSP1 than in SSP2 across all RCPs in 2050. Mostly falling between -4 and 3 log₁₀ particles per litre in SSP1 and -4 and 5 log₁₀ particles per litre in SSP2, monthly

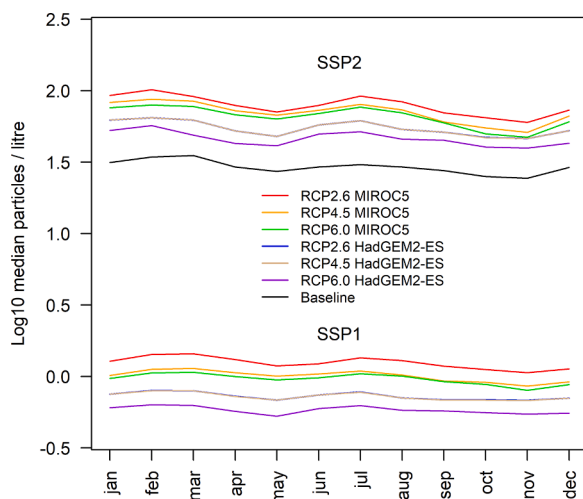


Fig. 3. Monthly Q50 rotavirus river concentrations for SSPs 1 and 2, and RCPs 2.6, 4.5 and 6.0 from two GCMs (HadGEM2-ES and MIROC5) simulated for 2050.

minimum and maximum concentration medians were simulated at -0.2 and 0.1 versus 1.6 and 1.9 rotavirus particles per litre in SSP1 and SSP2, respectively (Figure 3 and Figure S10). Although the GCM and RCP patterns in Figure 3 may be striking and resulting from variances in river discharge, there were limited overall output differences between RCPs and GCMs in SSP1 or in SSP2. The slightly reduced median concentrations from RCPs 2.6 to 6.0 for both GCMs was likely due to overall increasing comparative river discharge, producing a river dilution effect. Predicted increases and reductions of river discharge from the baseline in RCP 2.6 and 4.5 at the northwest and southwest of the country in HadGEM2-ES likely offset their influence on scenario rotavirus concentrations, thereby producing limited comparative differences. The spatially explicit results across the country show higher river contamination in SSP2 than in SSP1 (Figure 4).

In comparison to the baseline for all RCPs, SSP2 median concentrations from HadGEM2-ES and MIROC5 increased by between 44% and 75%, and mean concentrations were between 25% and 36% higher. Some differences between GCMs were also highlighted as more important than the differences between RCPs. For MIROC5 stronger increases were simulated than in HadGEM2-ES for both median and mean rotavirus concentrations, resulting from the discharge-related dilution in HadGEM2-ES. In contrast, in SSP1 all GCMs and RCPs showed strong rotavirus concentration reductions. The medians fell by between -100% and -121% and means by between -54% and -61%. Like in SSP1, across RCPs, GCM median and mean concentrations were lower in HadGEM2-ES than in MIROC5 when compared to the baseline. Detailed results are presented in Table S7.

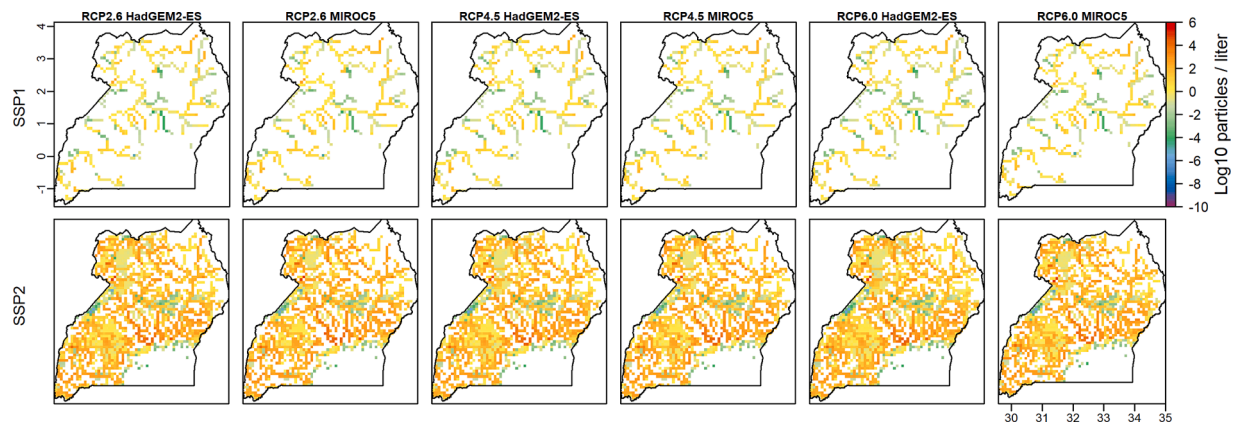


Fig. 4. Spatially-explicit mean annual rotavirus concentrations in Uganda's rivers in 2050 for SSPs 1 and 2 matrixed with RCPs 2.6, 4.5 and 6.0. RCPs are generated from two GCMs (HadGEM2-ES and MIROC5) at a $0.0833 \times 0.0833^\circ$ grid resolution.

4. Discussion

4.1. The GloWPa-Rota C2 model sensitivity

Our sensitivity analysis highlighted that strongly reducing K_{pit} and changes in prevalence and excretion rates of rotavirus influenced the simulated rotavirus concentrations the most.

Orner et al. (2019) argued that longer storage or emptying periods contribute more to microbial die-off than factors like pit storage temperature, pH and moisture content. The high K_{pit} and the consequent large rotavirus storage reductions achieved on site may explain the limited output correlation to changes in emptying frequencies. However, an emptying event much earlier than the baseline's 3 years likely mobilises more viable rotavirus particles. We tested the influence of a much shorter storage time from the baseline's once in 3 years to monthly and obtained 3 orders of magnitude increase in mean rotavirus concentrations. Interestingly, emptying frequencies may even be higher in densely populated areas or in non-household sanitation technologies (Schoebitz et al., 2017, 2016).

The uncertainty in rotavirus shedding is primarily due to limited epidemiological observations. Whenever present, rotavirus incidence and prevalence data are constrained by spatial variability, symptomatic and asymptomatic prognosis and inequities between hospitalization and health care access (Bwogi et al., 2016; Fuhrmann et al., 2016; Mwenda et al., 2010; Troeger et al., 2018). For instance, a study combined gastroenteritis from various pathogens, including rotavirus, of 10.9 (adults) and 8.3 (children) episodes per person per year for populations along an open-drain water system in Kampala (Fuhrmann et al., 2016). Another study compiled a national rotavirus incidence of 0.694 episodes per person per year from the Global Burden of Disease study (Troeger et al., 2018), likely representing populations along a polluted water system. Wastewater surveillance could be a better estimator of community faecal pathogen incidence and excretion levels. It could be an early warning tool, such as recently applied for the coronavirus disease (Ahmed et al., 2020; Medema et al., 2020). Nevertheless, high rotavirus incidence rates, particularly in children below 5 years, and the consequent excretion rates are primary drivers of rotavirus loading as observed in this and other studies (Ferguson et al., 2007; Okaali and Hofstra, 2018; Reder, 2017; Vermeulen et al., 2019).

4.2. Simulating baseline rotavirus river inputs: input data and assumptions

The results were influenced by model assumptions and input data uncertainties. As expected, illegal pit flushing in urban areas contributed the largest onsite sanitation share compared to the dumping on water, on land or from treated faecal sludge. Ratio assumptions for illegal faecal

sludge disposal were informed by literature and were considered representative for all urban areas, which may be unrealistic because of the possible faecal sludge management differences. The legally emptied-to-treatment faecal sludge loadings were largely reduced by the assumed steady-state K_{pit} , irrespective of the contemporary storage times, as shown by the sensitivity analysis. Although our sensitivity analysis shows limited influences of changes in illegal disposal ratios, fractions and emptying frequencies, the GloWPa model would benefit from formal and informal faecal sludge management field records. However, such data are not readily available because unregulated disposal activities are complex to document (Schoebitz et al., 2017).

A large section of Uganda's rural population uses onsite systems, where rotavirus particles were assumed to be safely contained. Rural open defecation inputs were dependent on surface runoff and the fraction of rotavirus land retention estimated from our literature review. Although the model was less sensitive to changes in land retention, robust approaches and data were limited in the literature. Grid cells with high runoff were crudely assigned low retention values and vice-versa. Landscape characteristics such as vegetation cover, physical and chemical soil properties were assumedly captured in the retention estimates. Davidson et al. (2016) correlated the decreasing recovery of rotavirus in surface runoff to vegetation cover, which further decreased virus particle soil infiltration. Therefore, using the data in Davidson et al. (2016) was our pragmatic choice.

4.3. Environmental survival and routing of rotavirus concentrations

Rotavirus river concentrations are dependent on environmental survival. Pancorbo et al. (1987) and Ward et al. (1986) showed that environmental survival and infectivity variably depend on virus type and matrix conditions. We focused on first-order rotavirus decay due to temperature and solar radiation in natural surface or representative waters; modelling both K 's using best-fitted log-linear relationships. Obviously, the available empirical literature requires updating. Although the derived K values may be uncertain, the sensitivity analysis showed that changes in temperature and sunlight dependent decay were of limited influence, and that rotavirus was relatively persistent in fresh surface waters. Additionally, despite not influencing model sensitivity and therefore uncertainty, it is likely that local characteristics in rivers such as euphotic water depth (z_{eu}) used to determine k_e and K_R vary from location to location. Notwithstanding, high river discharges such as $>100 \text{ m}^3\text{s}^{-1}$ seen from CWaTM (Figure S6), may translate into less residence time for reductions by K_T and K_R . Moreover, virus inactivation may not always be log-linear due to matrix conditions and antiviral agents producing shoulder, tailing or biphasic die-off kinetics (Abad et al., 1997; Pinon and Vialette, 2018). Kraay et al. (2018) positively correlated rotavirus decay to water temperature while determining

waterborne transmission between communities. However, their regression analysis generated limited significance to decay for a combination of natural, secondary effluent, distilled and sterilized water types. Moreover, die-off curves of most microbes are typically non-linear but can be approximated as a first-order exponential decay with characteristic decay, particularly under limited data, such as resulting from our literature reviews for K_T and K_R (González, 1995).

The GloWPa-Rota C2 routed rotavirus concentrations from low to high accumulation grids using input data within Uganda. Thus, border entry points were not specified and accounted for, because neighbouring-country input data was not used and river discharge was cropped within Uganda's borders. However, extended fluvial networks are often trans-border and mobilise various contaminants. Therefore, we identified 5 most important border grids and estimated river inputs introduced into each of the cells (Figure S9). Notably, the most important border grid is the single exit of Lake Victoria, with originally higher discharge values than the median, between 800 and 1500 m^3s^{-1} . Except for this grid, the model simulated loads and concentrations travelling downstream but running within the borders of Uganda where input data is available. The need to adjust for border inflows other than at the Lake Victoria exit point may currently not be necessary.

4.4. Rotavirus concentrations in 2050: changes in model output drivers

In 2050, rotavirus concentrations will be largely driven by population, urbanization and sanitation changes, rather than by hydrological inputs. In SSP2, more rotavirus contamination was mobilised when more people were using sewerage systems, while the adequately treated wastewater proportions remained largely unchanged. This means that stronger and more deliberate interventions will need to be adopted to reduce surface water loadings in SSP2 to SSP1 levels. In the latter scenario, treatment removal was improved by 3 logs in wastewater stabilization ponds, non-treatment was eliminated and all collected wastewater reached tertiary treatment in conventional systems.

Compared to historical data, RCP 6.0 was the most plausible medium climate scenario for the extended Lake Victoria basin and SSP2 suggested to lead towards RCP 6.0 in 2040 (Tramberend et al., 2020). However, GCMs may provide limited spatial variability for local regions such as below 200 km resolution at monthly or daily timesteps (Mendez et al., 2020). Averaging and exclusion of local features in GCMs may explain the limited differences between the RCP outputs in our study. The low-detailed spatial and temporal resolutions likely aggregate the hydrologic processes dynamics. Consequential uncertainty may therefore accumulate in the GloWPa-Rota C2 outputs. For instance, Vermeulen et al. (2019) found that a version of the GloWPa model simulated high *Cryptosporidium* concentrations in some larger rivers. Moreover, the current monthly GloWPa-Rota C2 output resolution does not include flash weather events such as floods. However, anticipated extremes of Uganda's climate towards drier or wetter seasons such as after 2050 may not directly translate into higher or lower pathogen loading into rivers. Similar model outcomes may also hold for neighbouring countries with projected seasonal precipitation variabilities (Gebrechorkos et al., 2019), where without strong improvements, future regional GloWPa-Rota C2 outputs may continue to be largely driven by population, urbanization, and sanitation coverage.

4.5. Performance and future potential of the GloWPa-Rota C2 model

Among others, one key approach towards building trust in models for data-poor areas and, therefore, in the GloWPa-Rota C2 model is to compare outputs with observational data (Strokal, 2016). Rotavirus is not regularly measured in Uganda's surface waters. However, a recent study measured rotavirus concentrations in an open drain wastewater system in Kampala (O'Brien et al., 2017). Average copies per litre ranged between 1.08×10^2 - 1.25×10^2 in a channel before a wastewater treatment plant, 4.22×10^2 - 3.77×10^3 in the influent, 1.87×10^2 -

3.72×10^3 in a channel after treatment and 6.49×10^1 - 2.99×10^2 in the draining swamp. These ranges fall within the GloWPa-Rota C2's baseline results, particularly closest to the median and mean of 1 and 2 \log_{10} particles per litre, respectively. Vermeulen et al. (2019) also simulated *Cryptosporidium* concentrations within the ranges of observed data for various global locations for their version of the GloWPa model. Our sensitivity analysis, Section 3.1, is another a step towards building model trust. It revealed that the GloWPa-Rota C2 model was largely less sensitive to nominal changes in most variables, except for pathogen incidence and excretion in faeces. This makes both the spatial and numerical outputs relatively reproducible and dependable, highlighting urban hotspot areas with predominant sanitation challenges. However, obtaining more spatial observation data will help to comprehensively validate the model.

Finally, besides sanitation improvement and water quality monitoring applications for SDG6.3, outputs of the GloWPa-Rota C2 could aid estimation of exposure risks and the resultant rotavirus diarrhoeal disease burden. With more detailed population, sanitation and hydrological data, the model could be applied to a local situation or even produce global outputs using country-level input data. Moreover, we could learn from various spatial- and temporal-scale influences generated from both input data types. Future scenarios could also examine the impacts of mass vaccination campaigns on concentrations and the diarrhoeal disease burden. The model could be applied to other bacteria, protozoa, virus, and helminths pathogens groups, like *Giardia*, *Salmonella*, cholera, norovirus, and hepatitis, although animal sources need to be considered where applicable.

5. Conclusions

The GloWPa-Rota C2 model simulated spatially explicit rotavirus river inputs and concentrations at subnational levels for Uganda from both onsite and offsite point and diffuse sanitation sources.

- Urban open defecation, treated wastewater effluent and the unsafe faecal sludge disposal contributed the largest shares to rotavirus river loadings for the baseline year 2015.
- Major hotspots of rotavirus contamination are the densely populated urban centres with predominant sanitation challenges typical in slum dwellings.
- The modelling framework showed that stronger and deliberate interventions including ending open defecation, safe management of faecal sludge, adequate wastewater treatment and reducing untreated proportions should be adopted, otherwise the rotavirus or similar pathogen loading into surface water will not be reduced.
- For future scenarios population growth, urbanization and inadequate sanitation are stronger contamination drivers than climate change.

To our knowledge, rotavirus rivers concentrations have been modelled for the first time, applied to Uganda but replicable elsewhere. Besides informing SDG6.3 progress monitoring, aiding sanitation service-level and microbial water quality management, simulated rotavirus concentrations can be inputs for quantitative microbial risk assessments under different exposure scenarios to attribute the burden of disease.

Declaration of Competing Interest

The authors declare that they have no known competing financial interests or personal relationships that could have appeared to influence the work reported in this paper.

Acknowledgements

This work was supported by the Knowledge-to-Practice - K2P project: Mapping and Implementing Knowledge to Practice Utilizing the Global

Water Pathogen Project (GWPP) funded by the Bill and Melinda Gates Foundation [OPP1180231].

Supplementary materials

Supplementary material associated with this article can be found, in the online version, at [doi:10.1016/j.watres.2021.117615](https://doi.org/10.1016/j.watres.2021.117615).

References

- Abad, F.X., Pintó, R.M., Villena, C., Gajardo, R., Bosch, A., 1997. Astrovirus survival in drinking water. *Appl. Environ. Microbiol.* 63, 3119–3122. <https://doi.org/10.1128/aem.63.8.3119-3122.1997>.
- Ahmed, W., Angel, N., Edson, J., Bibby, K., Bivins, A., O'Brien, J.W., Choi, P.M., Kitajima, M., Simpson, S.L., Li, J., Tschärke, B., Verhagen, R., Smith, W.J.M., Zaugg, J., Diereens, L., Hugenholz, P., Thomas, K.V., Mueller, J.F., 2020. First confirmed detection of SARS-CoV-2 in untreated wastewater in Australia: A proof of concept for the wastewater surveillance of COVID-19 in the community. *Sci. Total Environ.* 728, 138764 <https://doi.org/10.1016/j.scitotenv.2020.138764>.
- Berendes, D.M., Kirby, A.E., Clennon, J.A., Agbemabiese, C., Ampofo, J.A., Armah, G.E., Baker, K.K., Liu, P., Reese, H.E., Robb, K.A., Wellington, N., Yakubu, H., Moe, C.L., 2018. Urban sanitation coverage and environmental fecal contamination: Links between the household and public environments of Accra, Ghana. *PLoS One* 13, 1–19. <https://doi.org/10.1371/journal.pone.0199304>.
- Bishop, R.F., 1996. Natural history of human rotavirus infection. *Arch Virol Suppl.*
- Burek, P., Satoh, Y., Kahil, T., Tang, T., Greve, P., Smilovic, M., Guillaumot, L., Zhao, F., Wada, Y., 2020. Development of the Community Water Model (CWatM v1.04) – a high-resolution hydrological model for global and regional assessment of integrated water resources management. *Geosci. Model Dev.* 13, 3267–3298. <https://doi.org/10.5194/gmd-13-3267-2020>.
- Bwogi, J., Malamba, S., Kigozi, B., Namuwulya, P., Tushabe, P., Kiguli, S., Byarugaba, D. K., Desselberger, U., Iturriza-Gomara, M., Karamagi, C., 2016. The epidemiology of rotavirus disease in under-five-year-old children hospitalized with acute diarrhea in central Uganda, 2012–2013. *Arch. Virol.* 161, 999–1003. <https://doi.org/10.1007/s00705-015-2742-2>.
- Caceres, V.M., Kim, D.K., Bresee, J.S., Horan, J., Noel, J.S., Ando, T., Steed, C.J., Weems, J.J., Monroe, S.S., Gibson, J.J., 1998. A viral gastroenteritis outbreak associated with person-to-person spread among hospital staff. *Infect. Control Hosp. Epidemiol.* <https://doi.org/10.1086/647788>.
- Davidson, P.C., Kuhlenschmidt, T.B., Bhattarai, R., Kalita, P.K., Kuhlenschmidt, M.S., 2016. Overland transport of rotavirus and the effect of soil type and vegetation. *Water* 8, 78. <https://doi.org/10.3390/w8030078>.
- Ferguson, C., Croke, B.F.W., Beatson, P.J., Ashbolt, N.J., Deere, D.A., 2007. Development of a process-based model to predict pathogen budgets for the Sydney drinking water catchment. *J. Water Health* 5, 187–208.
- Ferguson, C., Husman, A.M.de R., Altavilla, N., Deere, D., Ashbolt, N.J., 2003. Fate and transport of surface water pathogens in watersheds. *Crit. Rev. Environ. Sci. Technol.* 33, 299–361. <https://doi.org/10.1080/10643380390814497>.
- Flato, G., Marotzke, J., Abiodun, B., Braconnot, P., Chou, S.C., Collins, W., Cox, P., Driouech, F., Emori, S., Eyring, V., Forest, C., Gleckler, P., Guilyardi, E., Jakob, C., Kattsov, V., Reason, C., Rummukainen, M., 2013. Evaluation of Climate Models, in: Stocker, T.F., Qin, D., Plattner, G.K., Tignor, M., Allen, S.K., Boschung, J., Nauels, A., Xia, Y., Bex, V., Midgley, P.M. (Eds.), *Climate Change 2013: The Physical Science Basis*. Cambridge University Press, Cambridge.
- Fleming, L.L., 2017. *A conceptual model of pathogen-specific hazards in pit latrines over time*. University of North Carolina at Chapel Hill.
- Frieler, K., Betts, R., Burke, E., Ciaisi, P., Denvil, S., Deryng, D., Ebi, K., Eddy, T., Emanuel, K., Elliott, J., Galbraith, E., Gosling, S.N., Halladay, K., Hattermann, F., Hickler, T., Hinkel, J., Huber, V., Jones, C., Krysanova, V., Lange, S., Lotze, H.K., Lotze-Campen, H., Mengel, M., Mouratiadou, I., Müller Schmied, H., Ostberg, S., Piontek, F., Popp, A., Reyer, C.P.O., Schewe, J., Stevanovic, M., Suzuki, T., Thonicke, K., Tian, H., Tittensor, D.P., Vautard, R., van Vliet, M.T., Warszawski, L., Zhao, F., 2016. Assessing the impacts of 1.5°C global warming – simulation protocol of the Inter-Sectoral Impact Model Intercomparison Project (ISIMIP2b). *Geosci. Model Dev. Discuss.* 1–59. <https://doi.org/10.5194/gmd-2016-229>.
- Fuhrmann, S., Winkler, M.S., Stalder, M., Niwagaba, C.B., Babu, M., Kabatereine, N.B., Halage, A.A., Utzinger, J., Cissé, G., Nauta, M., 2016. Disease burden due to gastrointestinal pathogens in a wastewater system in Kampala, Uganda. *Microb. Risk Anal.* 4, 16–28. <https://doi.org/10.1016/j.mran.2016.11.003>.
- Gebrechorkos, S.H., Hülsmann, S., Bernhofer, C., 2019. Regional climate projections for impact assessment studies in East Africa. *Environ. Res. Lett.* 14, 044031 <https://doi.org/10.1088/1748-9326/ab055a>.
- González, J.M., 1995. Modelling enteric bacteria survival in aquatic systems. *Hydrobiologia* 316, 109–116. <https://doi.org/10.1007/BF00016892>.
- Hofstra, N., 2011. Quantifying the impact of climate change on enteric waterborne pathogen concentrations in surface water. *Curr. Opin. Environ. Sustain.* 3, 471–479. <https://doi.org/10.1016/j.cosust.2011.10.006>.
- Hofstra, N., Bouwman, A.F., Beusen, A.H.W., Medema, G.J., 2013. Exploring global Cryptosporidium emissions to surface water. *Sci. Total Environ.* 442, 10–19. <https://doi.org/10.1016/j.scitotenv.2012.10.013>.
- Hofstra, N., Vermeulen, L.C., Derx, J., Flörke, M., Mateo-Sagasta, J., Rose, J., Medema, G. J., 2019. Priorities for developing a modelling and scenario analysis framework for waterborne pathogen concentrations in rivers worldwide and consequent burden of disease. *Curr. Opin. Environ. Sustain.* 36, 28–38. <https://doi.org/10.1016/j.cosust.2018.10.002>.
- IPCC, 2014. *Impacts, Adaptation, and Vulnerability: Contribution of working group II to the fifth assessment report of the Intergovernmental Panel on Climate Change*. Intergovernmental Panel on Climate Change.
- Katukiza, A.Y., Ronteltap, M., Niwagaba, C.B., Foppen, J.W.A.A., Kansime, F., Lens, P.N.L.L., 2012. Sustainable sanitation technology options for urban slums. *Biotechnol. Adv.* 30, 964–978. <https://doi.org/10.1016/j.biotechadv.2012.02.007>.
- Katukiza, A.Y., Ronteltap, M., van der Steen, P., Foppen, J.W.A., Lens, P.N.L.L., 2013. Quantification of microbial risks to human health caused by waterborne viruses and bacteria in an urban slum. *J. Appl. Microbiol.* 116, 447–463. <https://doi.org/10.1111/jam.12368>.
- Kayima, J.K., Kyakula, M., Komakech, W., Echimu, S.P., 2010. A study of the degree of Pollution in Nakivubo Channel, Kampala, Uganda. *J. Appl. Sci. Environ. Manag.* 12 <https://doi.org/10.4314/jasem.v12i2.55540>.
- Kirk, J.T.O., 1994. *Light and Photosynthesis in Aquatic Ecosystems*, illustrate. ed. Cambridge University Press, New York.
- Kirk, J.T.O., 1981. Monte Carlo study of the nature of the underwater light field in, and the relationships between optical properties of, turbid yellow waters. *Aust. J. Mar. Freshw. Res.* 32, 517–532. <https://doi.org/10.1071/MF9810517>.
- Kiulia, N.M., Hofstra, N., Vermeulen, L.C., Obara, M., Medema, G.J., Rose, J., 2015. Global occurrence and emission of rotaviruses to surface waters. *Pathogens* 4, 229–255. <https://doi.org/10.3390/pathogens4020229>.
- Kraay, A.N.M., Brouwer, A.F., Lin, N., Collender, P.A., Remais, J.V., Eisenberg, J.N.S., 2018. Modeling environmentally mediated rotavirus transmission: The role of temperature and hydrologic factors. *Proc. Natl. Acad. Sci.* 115, E2782–E2790. <https://doi.org/10.1073/pnas.1719579115>.
- Lee, Z.-P., Du, K., Arnone, R., 2005. A model for the diffuse attenuation coefficient of downwelling irradiance. *J. Geophys. Res.* 110, C02016. <https://doi.org/10.1029/2004JC002275>.
- Levy, K., Smith, S.M., Carlton, E.J., 2018. Climate change impacts on waterborne diseases: moving toward designing interventions. *Curr. Environ. Heal. Reports* 5, 272–282. <https://doi.org/10.1007/s40572-018-0199-7>.
- Mawdsley, J.L., Bardgett, R.D., Merry, R.J., Pain, B.F., Theodorou, M.K., 1995. Pathogens in livestock waste, their potential for movement through soil and environmental pollution. *Appl. Soil Ecol.* 2, 1–15. [https://doi.org/10.1016/0929-1393\(94\)00039-A](https://doi.org/10.1016/0929-1393(94)00039-A).
- McCormick, N.J., Høgerslev, N.K., 1994. Ocean optics attenuation coefficients: local versus spatially averaged. *Appl. Opt.* 33, 7067. <https://doi.org/10.1364/AO.33.007067>.
- Medema, G., Heijnen, L., Elsinga, G., Italiaander, R., Brouwer, A., 2020. Presence of SARS-Coronavirus-2 RNA in sewage and correlation with reported COVID-19 prevalence in the early stage of the epidemic in the Netherlands. *Environ. Sci. Technol. Lett.* 7, 511–516. <https://doi.org/10.1021/acs.estlett.0c00357>.
- Mendez, M., Maathuis, B., Hein-Griggs, D., Alvarado-Gamboa, L.F., 2020. Performance evaluation of bias correction methods for climate change monthly precipitation projections over Costa Rica. *Water* 12, 482. <https://doi.org/10.3390/w12020482>.
- Murungi, C., van Dijk, M.P., 2014. Emptying, Transportation and Disposal of faecal sludge in informal settlements of Kampala Uganda: The economics of sanitation. *Habitat Int* 42, 69–75. <https://doi.org/10.1016/j.habitatint.2013.10.011>.
- Mwenda, J.M., Ntoto, K.M., Abebe, A., Enweronu-Laryea, C., Amina, I., Mchomvu, J., Kisakye, A., Mpabalwani, E.M., Pazvakavambwa, I., Armah, G.E., Seheri, L.M., Kiulia, N.M., Page, N., Widdowson, M.-A., Steele, A.D., 2010. Burden and epidemiology of rotavirus diarrhea in selected African countries: preliminary results from the African Rotavirus Surveillance Network. *J. Infect. Dis.* 202 (Suppl), S5–S11. <https://doi.org/10.1086/653557>.
- O'Brien, E., Nakyazze, J., Wu, H., Kiwanuka, N., Cunningham, W., Kaneene, J.B., Xagorarakis, I., 2017. Viral diversity and abundance in polluted waters in Kampala, Uganda. *Water Res.* 127, 41–49. <https://doi.org/10.1016/j.watres.2017.09.063>.
- Okaali, D.A., Hofstra, N., 2018. Present and future human emissions of rotavirus and to Uganda's surface waters. *J. Environ. Qual.* 47, 1130. <https://doi.org/10.2134/jeq2017.12.0497>.
- Orner, K., Naughton, C., Stenstrom, T.-A., 2019. Pit Toilets (Latrines). In: Mihelcic, J., Verbyla, M. (Eds.), *Global Water Pathogen Project*. Michigan State University. <https://doi.org/10.14321/waterpathogens.56>.
- Pancorbo, O.C., Evanshen, B.G., Campbell, W.F., Lambert, S., Curtis, S.K., Woolley, T.W., 1987. Infectivity and antigenicity reduction rates of human rotavirus strain Wa in fresh waters. *Appl. Environ. Microbiol.* 53, 1803–1811. <https://doi.org/10.1128/AEM.53.8.1803-1811.1987>.
- Peal, A., Evans, B., Ahilan, S., Ban, R., Blackett, I., Hawkins, P., Schoebitz, L., Scott, R., Sleigh, A., Strande, L., Veses, O., 2020. Estimating safely managed sanitation in urban areas: lessons learned from a global implementation of excreta-flow diagrams. *Front. Environ. Sci.* 8, 1–13. <https://doi.org/10.3389/fenvs.2020.00001>.
- Pinon, A., Viallette, M., 2018. Survival of viruses in water. *Intervirology* 61, 214–222. <https://doi.org/10.1159/000484899>.
- Reder, K., 2017. *Large-Scale Modeling of Bacterial Contamination in Rivers, to Support the Global Assessment of Pollutant Concentrations in Rivers*. University of Kassel.
- Riahi, K., van Vuuren, D.P., Kriegler, E., Edmonds, J., O'Neill, B.C., Fujimori, S., Bauer, N., Calvin, K., Dellink, R., Fricko, O., Lutz, W., Popp, A., Cuaresma, J.C., KC, S., Leimbach, M., Jiang, L., Kram, T., Rao, S., Emmerling, J., Ebi, K., Hasegawa, T., Havlik, P., Humenöder, F., Da Silva, L.A., Smith, S., Stehfest, E., Bosetti, V., Eom, J., Gernaat, D., Masui, T., Rogelj, J., Strefler, J., Drouet, L., Krey, V., Luderer, G., Harmsen, M., Takahashi, K., Baumstark, L., Doelman, J.C., Kainuma, M., Klimont, Z., Marangoni, G., Lotze-Campen, H., Obersteiner, M., Tabeau, A., Tavoni, M., 2017. The Shared Socioeconomic Pathways and their energy, land use,

- and greenhouse gas emissions implications: An overview. *Glob. Environ. Chang.* 42, 153–168. <https://doi.org/10.1016/j.gloenvcha.2016.05.009>.
- Rodrigues, J., Acosta, V.C., Candeias, J.M.G., Souza, L.O., Filho, F.J.C., 2002. Prevalence of diarrheogenic *Escherichia coli* and rotavirus among children from Botucatu, São Paulo State, Brazil. *Brazilian J. Med. Biol. Res.* 35, 1311–1318. <https://doi.org/10.1590/S0100-879X2002001100008>.
- Schäfer, A., Ustohal, P., Harms, H., Stauffer, F., Dracos, T., Zehnder, A.J.B., 1998. Transport of bacteria in unsaturated porous media. *J. Contam. Hydrol.* 33, 149–169. [https://doi.org/10.1016/S0169-7722\(98\)00069-2](https://doi.org/10.1016/S0169-7722(98)00069-2).
- Schoebitz, L., Bischoff, F., Lohri, C., Niwagaba, C., Siber, R., Strande, L., 2017. GIS analysis and Optimisation of Faecal Sludge Logistics at City-Wide Scale in Kampala, Uganda. *Sustainability* 9, 194. <https://doi.org/10.3390/su9020194>.
- Schoebitz, L., Niwagaba, C.B., Strande, L., 2016. SFD Promotion Initiative Kampala Uganda Final Report. Eawag/Sandec.
- Strokhal, M., 2016. River Export of Nutrients to the Coastal Waters of China: the MARINA Model to Assess Sources, Effects and Solutions. University. <https://doi.org/10.18174/393126>.
- Tate, J.E., Burton, A.H., Boschi-Pinto, C., Parashar, U.D., 2016. Global, regional, and national estimates of rotavirus mortality in children <5 years of age, 2000–2013. *Clin. Infect. Dis.* 62, S96–S105. <https://doi.org/10.1093/cid/civ1013>.
- Tate, J.E., Rheingans, R.D., O'Reilly, C.E., Obonyo, B., Burton, D.C., Tornheim, J.A., Adazu, K., Jaron, P., Ochieng, B., Kerin, T., Calhoun, L., Hamel, M., Laserson, K., Breiman, R.F., Feikin, D.R., Mintz, E.D., Widdowson, M., 2009. Rotavirus disease burden and impact and Cost-effectiveness of a rotavirus vaccination program in Kenya. *J. Infect. Dis.* <https://doi.org/10.1086/605058>.
- Thomann, R.V., Mueller, J.A., 1987. *Principles of Surface Water Quality Modeling and Control*, Illustrate. ed., 1987. Harper & Row, New York.
- Tramberend, S., Burtscher, R., Burek, P., Kahil, T., Fischer, G., Mochizuki, J., Kimwaga, R., Nyenje, P., Ondiek, R., Nakawuka, P., Hyandy, C., Sibomana, C., Luoga, H.P., Matano, A.S., Langan, S., Wada, Y., 2020. East African community water vision. Regional scenarios for human - natural water system transformations. *SSRN Electron. J.* <https://doi.org/10.2139/ssrn.3526896>.
- Troeger, C., Khalil, I.A., Rao, P.C., Cao, S., Blacker, B.F., Ahmed, T., Armah, G., Bines, J. E., Brewer, T.G., Colombara, D.V., Kang, G., Kirkpatrick, B.D., Kirkwood, C.D., Mwenda, J.M., Parashar, U.D., Petri, W.A., Riddle, M.S., Steele, A.D., Thompson, R. L., Walson, J.L., Sanders, J.W., Mokdad, A.H., Murray, C.J.L., Hay, S.I., Reiner, R.C., 2018. Rotavirus vaccination and the global burden of rotavirus diarrhea among children younger than 5 Years. *JAMA Pediatr* 172, 958. <https://doi.org/10.1001/jamapediatrics.2018.1960>.
- Tsinda, A., Abbott, P., Chenoweth, J., 2015. Sanitation markets in urban informal settlements of East Africa. *Habitat Int* 49, 21–29. <https://doi.org/10.1016/j.habitatint.2015.05.005>.
- van Vliet, M.T., Flörke, M., Harrison, J.A., Hofstra, N., Keller, V., Ludwig, F., Spanier, J. E., Strokhal, M., Wada, Y., Wen, Y., Williams, R.J., 2019. Model inter-comparison design for large-scale water quality models. *Curr. Opin. Environ. Sustain.* 36, 59–67. <https://doi.org/10.1016/j.cosust.2018.10.013>.
- van Vuuren, D.P., Edmonds, J., Kainuma, M., Riahi, K., Thomson, A., Hibbard, K., Hurtt, G.C., Kram, T., Krey, V., Lamarque, J.-F., Masui, T., Meinshausen, M., Nakicenovic, N., Smith, S.J., Rose, S.K., 2011. The representative concentration pathways: an overview. *Clim. Change* 109, 5–31. <https://doi.org/10.1007/s10584-011-0148-z>.
- Vermeulen, L.C., Benders, J., Medema, G.J., Hofstra, N., 2017. Global cryptosporidium loads from livestock manure. *Environ. Sci. Technol.* <https://doi.org/10.1021/acs.est.7b00452>.
- Vermeulen, L.C., van Hengel, M., Kroeze, C., Medema, G.J., Spanier, J.E., van Vliet, M.T., Hofstra, N., 2019. Cryptosporidium concentrations in rivers worldwide. *Water Res* 149, 202–214. <https://doi.org/10.1016/j.watres.2018.10.069>.
- Ward, R.L., Knowlton, D.R., Winston, P.E., 1986. Mechanism of inactivation of enteric viruses in fresh water. *Appl. Environ. Microbiol.* 52, 450–459.
- WHO, UNICEF, 2017. Progress on Drinking Water, Sanitation and Hygiene: 2017 Update and SDG Baselines. Geneva.
- Williams, A.R., Overbo, A., 2015. Unsafe return of human excreta to the environment: a literature review.